

CUTHERMO: Understanding GPU Memory Inefficiencies with Heat Map Profiling

Yanbo Zhao*, Jinku Cui*, Zecheng Li*, Shuyin Jiao*, Xu Liu*, Jiajia Li*

*North Carolina State University

yzhao62@ncsu.edu, jcui23@ncsu.edu, zli94@ncsu.edu, sjiao2@ncsu.edu, xuliu88@ncsu.edu, jjajia.li@ncsu.edu

Abstract—GPUs have become indispensable in high-performance computing, machine learning, and many other domains. Efficiently utilizing the memory subsystem on GPUs is critical for maximizing computing power through massive parallelism. Analyzing memory access patterns has proven to be an effective method for understanding memory bottlenecks in applications. However, comprehensive runtime and fine-grained memory profiling support is lacking on GPU architectures. In this work, we introduce CUTHERMO, a lightweight and practical profiling tool for GPU memory analysis. It operates on GPU binaries without requiring any modifications to hardware, operating system, or application source code. Given a CUDA application, CUTHERMO identifies memory inefficiencies at runtime via a heat map based on distinct visited warp counts to represent word-sector-level data sharing and provides optimization guidance in performance tuning iterations. Through our experiments on six applications, we identified five memory access patterns that are portable across different GPU architectures. By evaluating optimization on two GPUs, CUTHERMO achieves up to 721.79% performance improvement.

I. INTRODUCTION

As GPUs become more and more powerful, an increasing number of applications leverage their parallel processing capabilities to accelerate computations across various domains, including scientific computing, artificial intelligence, and data analytics. With the exponential growth of data, memory- and data-intensive applications have become a major component of GPU workloads, necessitating efficient memory management and optimization strategies. Despite the growing accessibility of GPU programming frameworks such as CUDA [1] and OpenCL [2], effectively utilizing GPUs to achieve high application performance remains a significant challenge for developers. These challenges stem from the complex programming model, intricate memory hierarchy, and the difficulty of efficiently mapping computations to hardware resources.

Effectively utilizing low-latency memory resources, such as registers, shared memory, and caches, is important for an application’s performance. In particular, GPUs provide a configurable shared memory and L1 cache structure that shares the same physical space. This flexibility allows workloads to dynamically adjust cache behavior but also introduces additional complexity in performance tuning. Furthermore, the replacement policy of caches in modern GPUs is non-trivial and architecture-dependent [3], making it more difficult for programmers to predict cache behavior. The disparity in developers’ familiarity with hardware intricacies further exacerbates these challenges, creating a gap between low-level

memory optimization techniques and high-level application development. Understanding memory access patterns during runtime, especially for input-sensitive applications, is crucial, to discover inefficiencies not covered by static analysis.

To address memory optimization concerns, several GPU memory profiling tools have been developed. Vendor-provided profilers such as NVIDIA Nsight Compute [4] and Compute Sanitizer [5] offer insights into memory bandwidth utilization, cache hit/miss rates, and memory allocation inefficiencies. However, these tools primarily provide high-level statistics, lacking fine-grained insights or reasons into the behavior of individual memory accesses. Additionally, academic profiling tools have explored various aspects of memory efficiency. GVProf [6] detects redundant memory accesses, while CUDAAAdvisor [7] employs LLVM [8] instrumentation to analyze memory reuse distance and divergence. While valuable, these tools are either limited to static analysis, dependent on compiler-based instrumentation, or lack runtime correlation between memory accesses and performance bottlenecks.

DrGPUM [9] is a recent runtime profiler that introduces an object-centric approach to memory profiling, analyzing memory inefficiencies at both the macroscopic (object-level) and microscopic (intra-object) scales. It correlates memory inefficiencies with specific data objects and GPU API calls, providing actionable insights for developers. However, DrGPUM primarily focuses on identifying *memory wastage*, such as unused or overallocated memory, rather than cache inefficiencies. It lacks explicit support for visualizing fine-grained memory access patterns within the streaming multiprocessor (SM) cores, a critical aspect in diagnosing performance issues related to shared memory and L1 cache interactions.

Compiler-based optimization frameworks attempt to improve memory efficiency by restructuring memory accesses, yet they are inherently constrained by memory safety models and conservative optimization strategies. Unlike human programmers, who can make domain-specific adjustments, compilers often lack the runtime information necessary to make aggressive transformations that exploit GPU memory hierarchy effectively. For example, memory access coalescing and shared memory utilization are highly workload-dependent and may require heuristics or application-specific tuning that a static compiler cannot fully anticipate.

The limitations of existing profilers and optimization frameworks highlight the need for real-time, hardware-aware memory profiling to assist both developers and compilers in

understanding memory inefficiencies and making informed optimization decisions. However, to achieve this goal, three challenges need to be addressed.

Challenge 1: The traditional memory access counting method to represent hotness cannot identify inefficient memory access patterns. The memory access counting method uses the number of memory accesses for addresses or cache lines to indicate how frequently a specific memory region is accessed. However, frequency information alone cannot distinguish data-sharing behavior among threads or warps on GPUs. For example, it fails to differentiate whether a memory region is accessed frequently by a single thread or shared and accessed by multiple threads within the same warp or across multiple warps. As a result, detecting inefficient memory access patterns becomes challenging. **Since memory instructions are issued at the warp level, the number of distinct warps accessing a memory region serves as a reliable indicator of locality within a thread block.**

Challenge 2: The granularity of memory regions should accurately reflect real memory access behavior on the hardware. There are different granularities of memory regions to consider, such as word, sector, cache line, and data object levels. Data objects are too coarse-grained to capture diverse behaviors across different code regions or CUDA kernels. At the word-level granularity, it is challenging to represent data-sharing behavior among threads and capture coalescing information accurately to reflect actual memory transactions. In NVIDIA’s cache architecture, a cache line comprises 128 bytes and is divided into four 32-byte *sectors* [10] for cache management. When a memory instruction is issued, the coalescing process consolidates targeted memory regions into sector-aligned requests. **Sectors serve as the fundamental memory transaction units after hardware memory request coalescing, making sector-level memory access analysis critical for accurately diagnosing memory inefficiencies.**

Challenge 3: To collect the aforementioned information, nonselective trace collection generates massive and noisy traces, making accurate in-SM performance analysis impossible. An algorithm typically generates a large number of memory instructions, especially on GPUs, which execute massive numbers of threads, leading to an overwhelming trace volume. Additionally, traces from warps in different thread blocks share the same warp indexing information, polluting the trace data and making it difficult to accurately analyze program behavior. The sampling method must be carefully designed, as time-based sampling alone cannot effectively filter out noisy traces. **We introduce a thread block-sampling instrumentation strategy that records traces from only a single user specified thread block (default 0) as a representative, ensuring low runtime overhead while improving memory behavior modeling accuracy. And kernel sampling is also supported by a whitelist method to reduce overhead.**

We introduce CUTHERMO, a lightweight, runtime profiler that provides fine-grained insights into memory access behavior on NVIDIA GPUs, which records accessed warp_ids within a target threadblock in the word-sector level, to moni-

tor in-SM memory behavior. CUTHERMO implemented using NVIDIA’s NVBit [11] dynamic binary instrumentation framework, operates directly on compiled CUDA binaries, eliminating the need for source code modifications, recompilation, or additional compiler passes. This design ensures seamless integration into existing workflows, making it practical for both production environments and proprietary software.

In summary, this paper makes the following contributions:

- We propose a novel runtime metric for categorizing memory behavior in GPU applications, by introducing the concept of the memory heat map. (Section IV-A)
- We present a lightweight, modular tool that selectively samples memory instructions of a thread block to balance profiling accuracy and runtime overhead while providing extensibility to other GPU platforms. (Section IV-B)
- We address five inefficient memory access patterns: hot spots, abuse of shared memory, false sharing, memory misalignment, and strided memory access through the memory heat map, enabling developers to pinpoint optimization opportunities. (Section IV-C)
- We evaluate inefficiency insights and apply optimizations to four applications on two different GPUs, achieving 1.85% to 721.79% performance improvement. (Sections V and VI)

II. NVIDIA GPU BACKGROUND

Modern NVIDIA GPUs are designed for massively parallel workloads, making them essential in fields such as scientific computing, artificial intelligence, and real-time graphics rendering [12]. This section gives a brief overview of the thread hierarchy of its programming model, memory hierarchy, and the relationship between them.

A. Thread Hierarchy

From a programmer’s view, a single kernel in a CUDA program launches a grid [1] that contains multiple thread blocks [2], each thread block consists of multiple threads [3]. For an application to well utilize GPU’s massive parallelism, usually tens of thousands or more threads will be allocated [12]. From an architectural view, thread execution is organized into units called “warps” [4], each containing 32 threads that execute in a Single Instruction Multiple Threads (SIMT) fashion. The core of the execution model is the Streaming Multiprocessor (SM), depicted in Figure 1, which contains four sub-cores, including warp scheduler, execution units (CUDA cores, Tensor cores [13] and Special Function Units (SFU)), Load/Store units (LD/ST) and register files, and other components. The warp scheduler issues instructions to warps that are ready for execution. While thread blocks are assigned to SMs in a non-deterministic manner with their mapping abstracted from users, the scheduling may vary across different runs. However, each thread block is always assigned to a single SM within a given execution. In this work, we analyze in-block memory access behavior as a reliable indicator for predicting the performance of in-SM memory components.

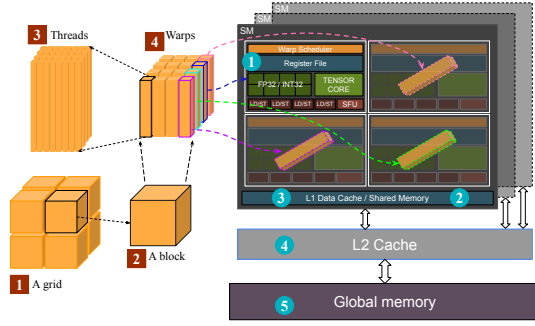


Fig. 1. An abstract architecture of NVIDIA GPUs.

B. Memory Hierarchy

The memory hierarchy commonly considered by CUDA programmers consists of registers (REG) ①, shared memory (SMEM) ②, L1 ③ and L2 ④ caches¹, and global memory (GMEM) ⑤. The global memory is the slowest but largest memory component on a GPU device with latency around 1000 cycles if TLB miss or 350 cycles if TLB hit [3]. L2 cache sits between SMs and the global memory, reducing latency to around 200 cycles and memory bandwidth pressure by caching frequently accessed data [3]. The memory hierarchy residing in an SM includes registers, shared memory and L1 cache. Registers provide the fastest access (1 cycle) and are private to each thread, and GPUs have a large amount of registers (such as 256KB per SM for Ampere GPUs). Shared memory and L1 cache share a configurable total size per SM (e.g., 128KB on `sm_86`). Though they both have low latency (around 25 cycles [3]) and are accessible to all threads within a thread block, shared memory is user-managed, while L1 cache is hardware-managed with around 20 cycles [3]. Each memory block is aligned to 128 bytes and divided into four 32-byte sectors [10] during data transfer between levels. The word size of NVIDIA GPUs is 32 bits (4 bytes).

GPUs use massive warps to effectively hide memory latency by overlapping computation with memory operations. Thus, efficient CUDA program execution depends on aligning memory access patterns well with the hardware’s capabilities. Coalesced global memory access and efficient utilization of shared memory contribute to improved application performance [14]. Comprehending the intricate balance between thread execution, memory access, and scheduling behavior is challenging. Even advanced developers find it difficult to write an efficient CUDA program that fully utilizes GPU resources, including computational power and high memory bandwidth. Moreover, NVIDIA GPU architecture continues to evolve and improve with each generation. But time evaluated micro-architectures persists. We deploy the *Word-Sector* granularity in this work to better abstract hardware behavior.

III. WORKFLOW OVERVIEW

CUTHERMO is designed to be a lightweight and practical profiling tool for GPU memory analysis, illustrated in Figure 2.

¹We refer to data caches in this paper.

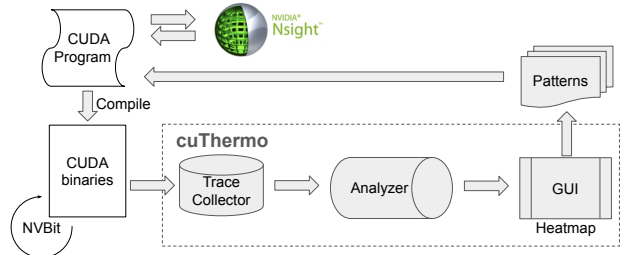


Fig. 2. The performance tuning workflow leveraging CUTHERMO.

It operates on GPU binaries without requiring any modifications to the hardware, operating system, or source code. Given a user’s CUDA code, CUTHERMO identifies its memory access inefficiencies and recognizes access patterns during runtime. The patterns will be used by users to optimize the corresponding region of their CUDA program. NVIDIA Nsight profiling tool can be used to testify the program behavior from a resource utilization perspective. Then the user could use CUTHERMO to detect the optimized version of the program again and check for other memory access inefficiencies, as the optimizing process iterates.

CUTHERMO consists of three major components: real-time trace collector, analyzer, and heat map visualization. Trace collector employs NVBit-based dynamic instrumentation to collect fine-grained memory access data along with metadata such as program counters, access sizes, and active thread masks in a CUDA application. To mitigate profiling overhead and noise, a thread block-sampling approach is used to ensure that memory access patterns remain representative while minimizing performance interference. Analyzer processes the memory access data collected at runtime to generate key statistics about GPU memory usage. It extracts word-level memory access information and computes the number of distinct warps that have accessed each word and sector, revealing patterns of memory locality and contention. The memory access logs are passed to the GUI visualization, where the memory footprints are aggregated and visualized as a heat map. The heat map highlights highly-shared memory regions, sparsely utilized sectors, and contention hot spots, providing developers with an intuitive way to diagnose performance bottlenecks.

These insights from CUTHERMO provide developers with a systematic approach to GPU memory optimization that remains portable across different GPU architectures. As fundamental memory hierarchy principles persist across GPU generations, hardware-aware optimizations from CUTHERMO’s heatmaps are transferable between GPU families.

IV. METHODOLOGY & IMPLEMENTATION

In this section, we introduce our heat map design and its construction techniques in CUTHERMO, then present five patterns that cannot be detected by the state-of-the-art tools.

A. Methodology

Recognizing different access patterns has a significant impact on performance optimization in GPUs. For example, frequently accessed data used by a single thread could be stored in registers (REG), which provide the fastest access

(refer to Section II). Unlike CPUs, NVIDIA GPUs have a much larger register resource, making it possible to store high-frequency, low-sharing, thread-private data efficiently. Without recognizing this pattern, those memory regions will unnecessarily occupy precious L1 cache space, which has a longer access latency than REG (refer to Section II), and will affect other data that genuinely requires L1 cache.

To detect inefficiencies in GPU memory, we define two essential components of a metric that are critical for revealing memory behavior: one captures the viewpoint that highlights inefficiencies, and the other defines the granularity that determines how the metrics are collected and organized.

Previous works [9], [15] use *memory access counts* to analyze memory behavior: the metric is the number of memory accesses, while the granularity is per-word memory address or per data-object, indicating how frequently a specific memory region is accessed. However, frequency information alone cannot distinguish data-sharing behavior among threads. For example, it fails to distinguish whether a memory region is accessed frequently by a single thread or simultaneously shared and accessed by multiple threads in one warp or even multiple warps. Other work [16] enhanced memory access count by classifying intra-warp and inter-warp instructions to detect data sharing between warps, but their approach fails to classify the level of sharing between threads. This approach can only determine whether a memory region is shared, not how it is shared.

Example. Figure 3 gives two different memory access patterns: perfect coalescing and false sharing [17] (explained in Section IV-C). In Figure 3(a), threads in a single warp access the same memory region, sector 00, once per thread. Its number of memory accesses is 1 for each word, 8 for the sector. However, the memory access count in Figure 3(b) is exactly the same with Figure 3(a) but in a different memory access pattern. Simply counting the number of memory accesses does not differentiate between these two access patterns.

To address the issue of access count measurement, we propose the number of distinct warps as the **METRIC**, which describes data sharing among warps, and two levels of memory **GRANULARITY**—words and sectors—to reflect actual data transformation. We refer to our metric-granularity table as a heat map to represent the “temperature” of fine-grained memory regions, thereby revealing elusive inefficiencies arising from algorithm design and the mismatch between software and GPU hardware.

1) *Metric—Distinct Warp Count:* GPU programming involves multiple levels of data sharing: among threads within the same warp, among threads from different warps within the same thread block, and among threads from different thread blocks. Different levels of sharing have varying memory access costs generally aligning with its corresponding memory hierarchies, aforementioned in Section II. Moreover, block binding varies across runs, making inter-block sharing unpredictable, except when data is extensively shared across all thread blocks. Thus, in this work, we focus on the first two levels of data sharing within the same thread block, which limits memory

optimization to resources available within an SM.

Since memory instructions are issued at the warp level, as noted in Section II, the number of distinct warps accessing a memory region serves as a reliable indicator of data sharing within an SM. Figure 3 illustrates the distinct warp count for perfect coalescing and false sharing patterns, respectively. In Figure 3(a), the words are accessed by threads within a single warp, forming a perfect coalescing pattern, resulting in a distinct warp count of 1. Conversely, in Figure 3(b), where the count is 8, eight distinct warps access different words in the sector, representing a false sharing pattern. The distinct warp count metric effectively describes the data-sharing level because it directly reflects the number of unique warp contributors, capturing the diversity of access patterns.

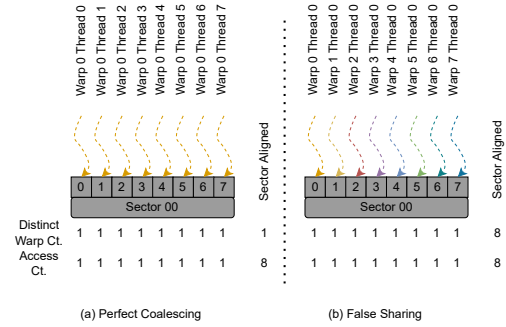


Fig. 3. Perfect coalescing vs. false sharing patterns in a GMEM sector. Our heat map can distinguish these two patterns, whereas the memory access counting method cannot.

2) *Granularity—Word-Sector:* The choice of granularity significantly impacts the detection of inefficiency patterns in memory operations. At the word-level granularity in the memory access counts method, analysis is restricted to determining whether an element is shared, offering limited insight. Sectors serve as the actual memory transaction units after hardware memory request coalescing. When a memory instruction is issued from a subcore to the LD/ST unit, the coalescing process consolidates targeted memory regions into sector-aligned requests, making data locality within a single instruction a key factor in determining actual memory transactions. As shown in Figure 3(a), a perfectly coalesced request from a single warp results in only one sector transaction. In contrast, false sharing in Figure 3(b) triggers eight sector transactions. However, if only the sector level is considered, the data sharing between words within a sector remains untraceable. To overcome these shortcomings, we record distinct warp counts at both the word and sector levels, enabling precise identification of the causes behind redundant memory transactions.

B. CUTHERMO Implementation

This section describes the three main components of CUTHERMO: Trace Collector, Analyzer, and GUI, which work together to construct and visualize the heat map, using distinct warp count as the metric and word-sector granularity to reveal memory behavior and identify memory inefficiencies. To support other GPU platforms, developers only need to

modify Trace Collector slightly to implement platform-specific instrumentation, and reuse other components.

1) *Trace Collector*: The Trace Collector consists of two main components: binary instrumentation and the trace packer. In the binary instrumentation phase, CUTHERMO captures the user’s execution command line and isolates the cubins from the target executable. It then parses these cubins with NVBit to inject our collection function at the appropriate locations by selecting the correct op code type (memory ops in CUTHERMO). This allows us to capture the associated attributes: pc, address, size, active_mask, access_flags, warp_id, and block_id, for all issued memory instructions. A description of these fields is provided below:

- 1) pc: Program counter.
- 2) address: A 32-element array of unsigned integers, recording all target addresses (global memory) accessed by this issued instruction within the warp.
- 3) size: The required length of the target address.
- 4) active_mask: Indicates active threads in the warp.
- 5) access_flags: Specify the access type and scope (e.g., load/store/atomic and shared/local/global).
- 6) warp_id: Warp index within a block, from 0 to 31.
- 7) block_id: Block index, used for block sampling.

In the trace packer, a GPU queue is created, containing a buffer and synchronizing flags to facilitate information transfer between the CPU and GPU. CUTHERMO packs the seven attributes for all issued memory instructions into the buffer and waits for the Analyzer to copy them to CPU memory as its input. *Trace Collector* also provides callback functions responsible for handling CUDA events, such as cudaMalloc (for global memory), cudaMallocManaged (for unified memory), kernel launch, and kernel end, to assist the Analyzer in organizing the collected trace.

Thread Block-Sampling. However, the trace size of a GPU application, even when limited to memory instructions, is too large to be stored entirely in GPU memory. More importantly, since identical warp IDs are reused across different blocks, this can lead to misinterpretation of memory access patterns, inefficiencies, and even make trace-based pattern detection impossible. To address this, we propose a thread block-sampling approach that collects the trace from only a single target thread block by including a bypass check in the injection function. Although simple, this method not only reduces collection overhead and thus makes CUTHERMO applicable to large applications, but also ensures accurate detection of memory access patterns by minimizing noise from other warps in different thread blocks.

2) *Analyzer*: The Analyzer maintains the status of synchronization flags in the GPU Queue and is responsible for transferring collected information between the CPU and GPU, then analyzing the collected traces to generate configuration files and CSV files that record heat maps. When a GPU Queue buffer is full, the Analyzer copies its contents to CPU memory and invokes the analyzing function to process the data. Additionally, the Analyzer implements memory registration

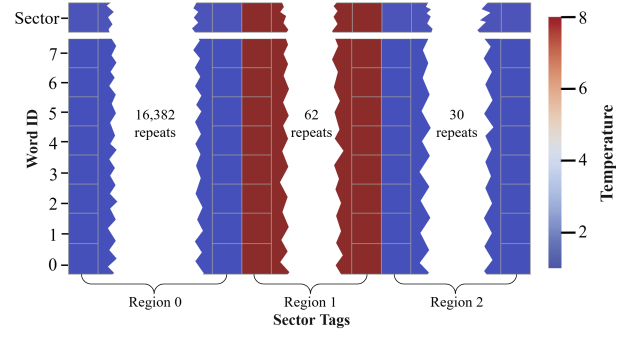


Fig. 4. Heat map using region indices and sector tags. Consecutive memory regions with identical temperatures are compressed, and the number of occurrences is indicated.

functions to store memory allocation information captured by the Trace Collector.

The Analyzer maintains a map, `sector_history_map`, using sector tags as keys and a size-9 array, `size_t[9]`, to record the history of distinct warp accesses. Every element is the bitmask to record the warp IDs into corresponding positions. The first eight elements of the value array represent each 4-byte word within the sector, while the last element represents the entire sector.

The analyzing function accepts a trace buffer grouped by warps, where each buffer element contains the aforementioned seven attributes, to fill in the `sector_history_map`. All the information other than address is shared over the threads within a warp when a memory instruction is issued. The addresses are then processed to obtain the sector tags, each of which denotes the starting address of a sector. Since the sector size is 32 bytes, the tag is calculated as $\text{sector tag} = \text{address}/32$ and the word offset within a sector as $\text{offset} = \text{address}\%32$. The corresponding entry in `sector_history_map` is updated by using $1 \ll \text{warp_id}$ and applying the bitwise OR ($|=$) operation with the bitmask in `sector_history_map[tag][offset]` and `sector_history_map[tag][8]`, thereby storing all accessed warp IDs for all the eight words and the entire sector.

After all traces of a kernel have been analyzed and kernel execution has ended, a flush function is invoked to count the number of 1s in the bitmasks of every entry in `sector_history_map`. These 1s represent the number of distinct warps that have accessed each word and each sector, and they are recorded in CSV files. Next, the start and end addresses of memory regions, along with the start and end sector tags, are stored in configuration files.

3) *Heat Map Visualization.*: Based on the configuration and CSV files generated by the Analyzer, CUTHERMO produces heat maps to visually represent memory access patterns. The CSV files provide the raw data for constructing the heat map, while configuration files map each memory sector to its corresponding region, allowing users to distinguish between different access patterns across regions.

Figure 4 illustrates the heat map design, where memory access patterns are categorized based on *region indices* while retaining sector tags for detailed access tracking. The hor-

horizontal axis represents sector tags, while the vertical axis corresponds to word IDs, indexing each word within a sector. The color intensity in each cell represents the *temperature*, indicating the number of distinct warps accessing a given sector—a higher temperature reflects greater memory sharing. An additional cell at the top of each sector represents the aggregated temperature of the entire sector, showing the total number of distinct warps that have accessed it. To enhance readability, consecutive memory regions with identical access patterns are grouped and labeled with their repetition count. A color-coded legend on the right uses a gradient of hues to visualize sector temperatures.

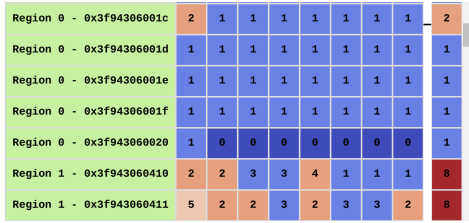
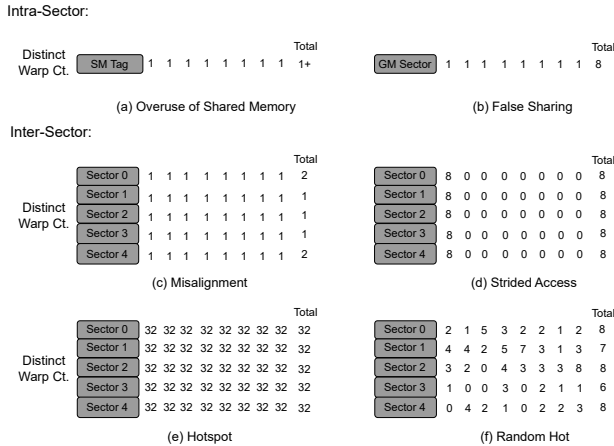


Figure 5 presents a screenshot of the heat map in CUTHERMO’s user interface. The visualization adopts a *vertical layout* to improve navigation and facilitate pattern recognition. The vertical scrolling feature allows users to scan through the memory access patterns efficiently, making it easier to pinpoint optimization opportunities at a glance.



C. Identified Patterns

(Random) Hot Spots. Hot sectors are identified by high temperatures in each word of certain sectors, and the sector temperature is close to the highest in its words. Figure 6(e) is a typical example of hot sectors which are accessed by 32 warps. Figure 6(f) is a case of random hot pattern, which shows random numbers of warps sharing the words.

Memory False Sharing. A warp performs a hardware coalescing process that merges memory access instructions from the same warp into sector-aligned memory transactions, after instructions have been issued. Thus, the memory access requests to different words of a sector will only cause 1 actual sector transaction within one warp. However, memory access instructions from multiple warps cannot take advantage of coalescing, thus leading to 8 sector transactions. This pattern of false sharing [17] on GMEM limits the application performance. Our heat map identifies this pattern, shown in Figure 6(b), where each word is accessed by one distinct warp, triggering multiple sector transactions from GMEM. The false sharing pattern differentiates from the hot spot pattern by the total number of distinct warps accessing an entire sector versus those accessing individual words within that sector. When false sharing occurs, the whole sector’s temperature is significantly higher than any single word within that sector.

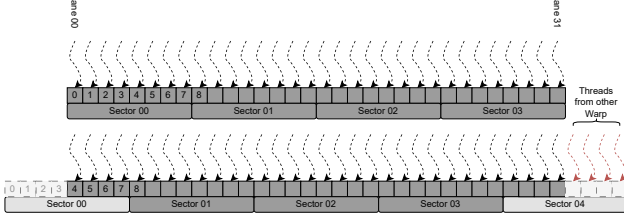


Fig. 7. Misaligned memory request. Five sectors need to be loaded into the L1 cache for warp 1, but the first and last four elements in sectors 0 and 4 will never be used.

in a 128-byte memory region show normal behavior where the threads in one warp access different words of a sector. However, the two boundary sectors 0 and 4 have two warps accessing words 4-7 and words 0-3 respectively, leading to one more sector transaction (5 vs. 4) from global memory to L1 cache and a waste of L1 cache due to semi-utilized sectors. Even though modern GPUs have powerful hardware components [10] that can handle irregular memory access patterns, those patterns still cause significant increases in memory request amounts and result in the inability to capture benefits by using built-in vectorized types. However, the extra sector transaction cannot be revealed from memory access counting because the memory access is always 8 for a sector. **Strided Memory Access.** Strided memory access refers to a memory access pattern in which consecutive threads access memory locations that are spaced apart by a fixed stride, rather than accessing contiguous locations. As shown in Figure 6(d), eight warps access the same word location across five sectors, with a stride size of 7. Seven out of eight words in each sector are never accessed by any warp during execution, meaning that 7/8 of the memory transactions are wasted. Additionally, the accessed words record a distinct warp count of 8, indicating that memory coalescing does not apply. This strided access pattern also wastes L1 cache due to a large number of unused words, reducing the available L1 cache for other data objects.

V. EVALUATION

This section evaluates our work from three perspectives: the patterns identified in real applications and benchmarks via CUTHHERMO, as well as the tool’s overhead and portability.

We evaluate CUTHHERMO on an x86_64 system equipped with an AMD Ryzen Threadripper PRO 5955WX 16-core processor and an NVIDIA Ada Lovelace RTX4090 GPU. The following system software is used: Linux 5.15.0-131-generic, NVIDIA CUDA Toolkit 12.1.r12.1, NVIDIA Driver 535.183.01, NVBit 1.7.3, and GCC 11.4.0.

Patterns in Applications. We use CUTHHERMO to detect the patterns described in Section IV-C within real applications and benchmark suites across five domains. The memory access patterns and their corresponding data objects from six applications and their kernels are listed in Table I as representatives.

General Matrix-Matrix Multiplication (**GEMM**), a fundamental operation in linear algebra, is widely used in scientific computing and machine/deep learning. Its kernels, `gemm_v00` and `gemm_v01` [19], exhibit hot spots and false sharing

TABLE I
REPRESENTATIVE MEMORY ACCESS PATTERNS DETECTED BY CUTHHERMO IN FIVE APPLICATIONS ACROSS MULTIPLE DOMAINS.

Domain	Application	CUDA Kernel	Data Object	Access Pattern
Linear Algebra	GEMM	<code>gemm_v00</code>	A	Hot
			B	False shared
		<code>gemm_v01</code>	C	False shared
			B	Hot
	SpMV	<code>spmv_csr</code>	rowOffsets	Misaligned
			x	Hot-random
Tensor Algebra	PASTA	<code>spt_TTMRankRBNnzKernelSM</code>	Y_shr	Abused SMEM
Solver	GRAMSCHM	<code>kernel2</code>	q	Strided
		<code>kernel3</code>	r	Strided, hot
Compression	cuSZp	<code>cuSZp_(de)compress_kernel_*</code>	exel_sum base_idx	Abused SMEM
Molecular Dynamics	GPUMD	<code>find_cell_counts</code>	cell_count	Strided, false shared
		<code>find_cell_contents</code>	cell_count cell_count_sum	

patterns. Sparse Matrix-Vector Multiplication (**SpMV**) [20] is a sparse linear algebra operation that efficiently processes matrices with mostly zero elements by storing only nonzero values in compressed formats. The `spmv_csr` kernel exhibits a misalignment pattern when accessing row pointers (`rowOffsets`) and a hot but random memory access pattern in vector `x`. **PASTA** [21], a Parallel Sparse Tensor Algorithm benchmark suite, is designed to evaluate sparse tensor algebra on different computer systems. The kernel `spt_TTMRankRBNnzKernelSM` exhibits a shared memory abuse pattern on `Y_shr` object. **GRAMSCHM** is a benchmark obtained from the PolybenchGPU suite [22], implementing the Gram-Schmidt algorithm on GPUs. The `kernel3` exhibits strided memory access and hot spot patterns on the data object `q`. **cuSZp** [23] is an ultra-fast, error-bounded GPU lossy compressor. The two data objects, `exel_sum` and `base_idx`, in kernels prefixed with `cuSZp_(de)compress_kernel_` exhibit shared memory abuse pattern. **GPUMD** [24] is a highly efficient, general-purpose molecular dynamics (MD) package widely used in the physics and chemistry communities. The kernels `find_cell_counts` and `find_cell_contents` exhibit strided and false sharing patterns in `cell_count` and `cell_count_sum`. The observed patterns reveal potential inefficiencies in these applications, motivating the kernel optimizations detailed in our case studies in Section VI, with the resulting performance improvements summarized in Table III.

TABLE II
PROFILING OVERHEAD OF CUTHHERMO AND NSIGHT COMPUTE (NCU).

Application	Runtime (Seconds)			Overhead	
	Original	CUTHHERMO	NCU	CUTHHERMO	NCU
GEMM	0.27	2.61	1.64	9.86×	6.20×
SpMV	1.19	1.36	2.08	1.14×	1.75×
PASTA	3.38	3.62	5.07	1.07×	1.50×
GRAMSCHM	1.35	77.90	1022.52	57.53×	755.19×
cuSZp	3.83	7.54	7.99	1.97×	2.08×
GPUMD	0.29	4.23	16.90	14.49×	57.90×

CUTHHERMO Overhead. We evaluate and compare the performance overhead of our CUTHHERMO (trace-based) and NVIDIA Nsight Compute (NCU, counter-based) on all the applications in Table II. We measure the average end-to-end execution time over 10 runs for the original application, the application running with CUTHHERMO, and the application

profiled using NCU with all memory metrics enabled. The last two columns of Table II report the overhead of CUTHERMO and NCU. In all studied applications, the overhead of CUTHERMO is significantly lower than that of NCU, because CUTHERMO only samples trace from one block per kernel launch, which will only generate at most 1024 threads’ memory trace. CUTHERMO also supports kernel sampling, similar to NCU; we enabled the kernel sampling in both CUTHERMO and NCU in overhead comparison for fairness. The target kernel list contains the inefficient kernels we found in Table I.²

For the SpMV, PASTA, cuSZp applications, the overhead remains relatively modest, ranging from $1.07\times$ to $1.97\times$, indicating an additional execution time of 7%–97%. However, GEMM exhibits significantly higher overheads of $9.86\times$ and $6.20\times$ for CUTHERMO and NCU, respectively. This substantial overhead arises because GEMM generates a large number of memory access requests, proportional to its computational complexity. As a result, the overhead of a trace-based tool like CUTHERMO increases accordingly. In contrast, NCU incurs a relatively lower overhead growth rate in GEMM because, as a hardware counter-based profiler, it collects metrics directly from hardware and drivers with a fixed overhead related to the duration of the kernel execution. And the overhead of GRAMSCHM and GPUMD is more related to the number of kernel launches rather than the memory access amounts.

TABLE III
PERFORMANCE IMPROVEMENT IN A4500 AND RTX4090 GPUS.
MEASURED IN CYCLES BY NCU.

Application	CUDA Kernel	Performance Improvement	
		A4500	RTX4090
GEMM	gemm_v00	721.79%	682.82%
	gemm_v01	26.07%	20.27%
SpMV	spmv_csr	1.85%	1.97%
PASTA	spt_TTMRankRBNnzKernelSM	163.56%	159.62%
GRAMSCHM	kernel2	4.51%	9.19%
	kernel3	23.18%	19.81%

Portability. CUTHERMO can detect memory access patterns and provide insights regardless of the NVIDIA GPU generation, as long as the sector-based memory system is used. We evaluate these insights and select four applications from studied applications on an NVIDIA Ada Lovelace RTX 4090 GPU, the one CUTHERMO deployed, and verify its portability on an NVIDIA Ampere RTX A4500 card in Table III.³ Both GPUs show reasonable performance speedup, proving the insights we found are true inefficiencies and our optimization guidance is portable among different GPU architectures. Table III shows similar speedup results on both the A4500 and RTX 4090, ranging from 1.85% to 721.79% and 1.97% to 682.82% respectively using the same optimization methods.

²The SpMV application operates on a $36,417 \times 36,417$ sparse matrix with 2,190,591 nonzeros [25], while PASTA processes a $154,985 \times 48,476 \times 76,728 \times 94,578$ tensor with 349,808 nonzeros [26]. cuSZp uses its built-in benchmark input, and GEMM executes matrix multiplication on two 1024×1024 square matrices. NCU use kernel replay mode (default).

³GPUMD and cuSZp are not included in the speedup evaluation because GPUMD requires domain experts for valid optimization, and the inefficient code snippet in cuSZp introduces only a 0.16% increase in instructions. Detail of cuSZp is discussed in Section VI.

VI. CASE STUDY

We showcase five applications that exhibit the four actionable inefficiency memory access patterns identified in Section IV-C. In this section, we focus on optimizing these applications and demonstrate the performance and efficiency improvements achieved through our optimizations. This highlights the importance of using CUTHERMO to identify inefficiencies and apply corrective measures.⁴ However, due to effective performance optimization in real-world applications often requiring extensive domain knowledge, we anticipate further performance gains can be achieved when deployed by domain experts using CUTHERMO.

```

1 --global__ void gemm_v00(m, n, k, alpha, A, lda, B, ldb, beta, C, ldc){
2   size_t C_row_idx{blockIdx.x*blockDim.x+threadIdx.x};
3   size_t C_col_idx{blockIdx.y*blockDim.y+threadIdx.y};
4   if (C_row_idx < m && C_col_idx < n) {
5       T sum(0);
6       for (size_t k_idx(0); k_idx < k; ++k_idx)
7           sum+=A[C_row_idx*lda+k_idx]*B[k_idx*ldb+C_col_idx];
8       C[C_row_idx*ldc+C_col_idx]=alpha*sum+beta*C[C_row_idx*ldc+C_col_idx];
9   }

```

Listing 1. gemm_v00 kernel. Every thread will calculate one element in C.

A. GEMM - False Sharing

General Matrix-Matrix Multiplication (GEMM) is a fundamental operation in linear algebra that multiplies two matrices to produce a third one. We study GEMM using a public GitHub repository [19] that contains multiple widely used optimization methods. We select the kernels `gemm_v00` and `gemm_v01` to identify and explain the *False Sharing* pattern and its optimization.

In the `gemm_v00` kernel (illustrated in Listing 1), each thread accesses matrices A and B and updates the result matrix C using `C_row_idx` (computed as `blockIdx.x * blockDim.x + threadIdx.x`) and `C_col_idx` (computed as `blockIdx.y * blockDim.y + threadIdx.y`). Due to the column-major access pattern of B, threads in the same iteration often fetch data spanning multiple 32-byte cache sectors, while each thread utilizes only a small portion (e.g., 4 bytes for a single-precision floating-point number). This results in significant memory waste—up to 7/8 of the sector’s data—since adjacent threads do not fully utilize the fetched memory, even though some reuse may occur later.

The heat map generated by CUTHERMO reveals a perfect match with the *False Sharing* pattern in matrices B and C. Kernel `gemm_v01` solved this inefficiency by swapping `C_row_idx` and `C_col_idx`, enabling threads within a warp to access contiguous memory regions. This adjustment improves alignment with the 32-byte sector granularity, maximizing the use of loaded sectors. By reassigning thread indices, the optimization reduces wasted memory bandwidth, ensuring more efficient sector utilization. Despite `gemm_v01` exhibiting a slightly lower L1 cache hit rate (94.93% vs. `gemm_v00`’s 99.22%) with the same number of instructions, it achieves $7.21\times$ and $6.83\times$ speedups on the A4500 and RTX 4090 GPUs, respectively.

⁴For pattern Hot and Random Hot, the optimization suggestion is placing those memory regions into SMEM, this optimization is well-known so we do not discuss it in this paper.


```

1 __global__ void spt_TTMRankRBNnzKernelSM(Y_val, Y_stride, Y_nnz, X_val,...){
2   extern __shared__ sptValue mem_pool[];
3   sptValue * const Y_shr = (sptValue *) mem_pool;
4   ...
5   for(sptIndex l=0; l<num_loops_r; ++l){
6     ...
7     for(sptNnzIndex nl=0; nl<num_loops_nnz; ++nl){
8       ...
9       int y_id= tidy * Y_stride + tidz; Y_shr[y_id] = 0;
10      __syncthreads();
11      if(x < Y_nnz){
12        ...
13        for(i = inz_begin; ...){
14          ...
15          Y_shr[y_id] += X_val[i] * U_val[row * U_stride + r];
16        }
17        __syncthreads();
18        Y_val[x * Y_stride + r] = Y_shr[y_id];
19        __syncthreads();
20      }
21    }
22 }

```

Listing 2. A sparse tensor-times-matrix kernel from PASTA, using shared memory to accelerate temporary results.

B. PASTA - Abuse of Shared Memory (Thread Local)

PASTA [21] is a parallel sparse tensor algorithm benchmark suite designed to help users evaluate the performance of different computer systems in sparse tensor algebra computations. We select the `spt_TTMRankRBNnzKernelSM` kernel (illustrated in Listing 2) for sparse tensor-times-matrix computation to discuss the *Abuse of Shared Memory* pattern.

This CUDA kernel suffers from a major inefficiency in its use of SMEM. The primary issue is that `Y_shr` is used to store per-thread computation results that do not actually need to be shared, leading to unnecessary memory operations and synchronization points. Using CUTHermo, we observe the *Abuse of Shared Memory* pattern.

To resolve this issue, we replace the SMEM usage with simple register variables (e.g., `sptValue local_sum = 0;`) to allow each thread to accumulate its results independently. This eliminates the need for SMEM allocation and most synchronization barriers. The only necessary global memory write occurs at the end of the computation, directly updating `Y_val`. This optimization achieves a $1.64\times$ and $1.60\times$ performance speedup on the A4500 and RTX 4090 GPUs, respectively.

C. cuSZp - Abuse of Shared Memory (Warp Local)

cuSZp is an ultra-fast, error-bounded GPU lossy compressor implemented in CUDA. It exhibits a similar pattern to PASTA, as all eight kernels prefixed by `cuSZp_compress_kernel_` and `cuSZp_decompress_kernel_` use SMEM to perform broadcasting within a warp. The key difference between PASTA and cuSZp lies in the level of data sharing. PASTA has no data sharing at all, whereas cuSZp shares data among threads within a warp. The insight here is that SMEM should not be used for in-warp data sharing.

To resolve this issue, we replace the use of SMEM for `exel_sum` and `base_idx` with registers and instead use warp-level intrinsics, such as `__shfl_sync(0xffffffff, exel_sum, srcLane)`. Additionally, we remove the related synchronization function calls. In this case, the corresponding inefficient lines will only be executed once which makes them hard to observe via cycles, but they can be detected by executed instruction counts. Our optimization eliminates all SMEM usage in the kernels, leading to 6.44% reduction in `stall_short_scoreboard` cycles.

```

1 __global__ void gramschmidt_kernel3(ni,nj,a,r,q,k){
2   int j = blockIdx.x * blockDim.x + threadIdx.x;
3   if ((j > k) && (j < _PB_NJ)){
4     r[k*NJ + j] = 0.0;
5     for (int i = 0; i < _PB_NI; i++){
6       r[k*NJ + j] += q[i*NJ + k] * a[i*NJ + j];
7     }
8     a[i*NJ + j] -= q[i*NJ + k] * r[k*NJ + j];
9   }

```

Listing 3. A kernel from PolybenchGPU, array `q` accessed by column major. Only $1/NJ$ part of array `q` will be accessed.

D. GRAMSCHM - Strided Access

GRAMSCHM, obtained from the PolybenchGPU benchmark suite [22], is a CUDA implementation of the Gram-Schmidt algorithm, which is commonly used for matrix orthogonalization. In `kernel3` (illustrated in Listing 3), each thread accesses elements of the `q` array in a strided pattern via `q[i*NJ+k]`, where consecutive memory accesses are separated by entire rows. This pattern prevents coalesced memory access, a critical factor for GPU performance.

The inefficiency stems from non-coalesced loads, where a single memory transaction cannot satisfy multiple threads in a warp. Although all threads require the same `q[i*NJ+k]` element, accessing `q[(i+1)*NJ+k]` in subsequent iterations requires jumping `NJ` elements away. This strided pattern prevents loop unrolling benefits since elements are not adjacent, leading to multiple separate memory transactions and significantly reduced memory bandwidth utilization. Using CUTHermo, we observe that only one word in each sector is accessed, and this word is shared by multiple warps, fitting the *strided access* pattern.

We fix this issue by transposing the `q` array’s indices to enable coalesced memory access, allowing threads within a warp to access adjacent memory locations simultaneously. This optimization improves memory transaction efficiency by enhancing intra-warp sector sharing while reducing inter-warp conflicts. The results show a $1.20\times$ speedup, a 7.69% reduction in register usage (from 26 to 24), and 20.05% fewer instructions with no precision loss on RTX 4090. On A4500, the optimization achieves a $1.23\times$ speedup, 18.16% fewer instructions, and the same reduction in register usage.

```

1 __global__ void spmv_kernel(numRows, rowOffsets, colIndices, values, x, y) {
2   int r = blockIdx.x * blockDim.x + threadIdx.x;
3   if (r < numRows) {
4     float sum = 0.0f;
5     for (int i=rowOffsets[r]; i<rowOffsets[r+1]; ++i){
6       int col = colIndices[i];
7       sum += values[i] * x[col];
8     }
9     y[row] = sum;
10  }

```

Listing 4. SpMV implementation based on the CSR format.

E. SpMV - Misalignment

Sparse Matrix-Vector Multiplication (SpMV) [20] is a fundamental kernel in scientific computing that efficiently processes matrices with mostly zero elements by storing only nonzero values in compressed formats such as the popular CSR format, which utilizes the `rowOffsets`, `colIndices`, and `values` arrays.

The SpMV algorithm (shown in Listing 4) suffers from misaligned memory access when threads read `rowOffsets[row+1]`. Since `rowOffsets` is of type `int` (4 bytes), this misalignment forces each warp to load 5

memory sectors instead of the optimal 4, resulting in a 25% overhead in memory transactions and index calculations.

Our optimization restructures the `rowOffsets` array by introducing duplicated storage in a zigzag pattern during preprocessing, enabling vectorized memory loads via `ldg.s32.v2` instructions. This optimization achieves a 1.85% and 1.97% speedup with 0.29% and 0.21% fewer instructions on A4500 and RTX 4090, respectively.

F. cuSPARSE - Closed-Source Library

By the methodology and implementation of CUTHERMO, we can also apply CUTHERMO to closed-source libraries, and deploy our observation to understand inefficiencies without access to the source code. We use CUTHERMO to analyze multiple cuSPARSE kernels, identifying *Abuse of Shared Memory*, *False Sharing*, and *Memory Misalignment* patterns within `matrix_scalar_multiply_kernel` and `load_balancing_kernel` from `sppm_csr`. Due to the closed source nature of cuSPARSE, we cannot provide specific code examples or optimizations, but this case shows the capacity of identifying inefficiencies in closed source libraries with CUTHERMO.

G. Discussion

CUTHERMO, based on instrumentation techniques, has both limitations and advantages. Its limitations include a reliance on vendor-provided binary instrumentation frameworks, which currently restricts platform compatibility, though its modular design enables easy deployment once the necessary framework components are available. Furthermore, it lacks an automatic pattern detection mechanism, as some memory inefficiencies are complex and require human judgment; instead, it offers a GUI for users to visualize memory access patterns and select from common ones. Additionally, it doesn't guarantee the selection of the most representative code block, instead allowing users to specify the block to sample and providing an interface for other profiling tools to identify representative blocks. However, a key advantage is its introduction of a novel metric for observing memory access patterns. For long-term maintainability, a lightweight alternative implementation, `cuThermo_light`, which relies solely on the NVBit framework, is provided, reducing external dependencies and ensuring sustained functionality across future GPU generations.

VII. RELATED WORK

Detecting and optimizing GPU memory inefficiencies remains a persistent challenge throughout the lifecycle of GPU application development. Numerous profiling and optimization techniques have been introduced to assist developers in tuning their kernels by reducing memory usage, identifying redundancies, recognizing memory access patterns, and evaluating locality characteristics.

A. Memory Redundancies

Instruction Redundancies: Several works have been proposed to identify redundant memory instructions in CPU and

GPU applications. *RedSPY* [27] and *LoadSPY* [28], leverage vendor-provided binary rewriters, hardware performance monitoring units, and debug registers to detect redundant memory instructions in CPUs. *DARSIE* [29] eliminates conditionally redundant memory instructions at the grid, block, and warp levels, providing insights into reducing executed instruction counts. However, these methods rely on specific hardware and software support or require custom simulators based on modified ISAs, limiting their applicability to real GPUs.

Value Redundancies: While tools like *Gvprof* [6] and *ValueExpert* [30] identify valuable runtime redundancies based on data values, they may not capture inefficiencies rooted in algorithmic structure or memory access patterns, which is the primary focus of our work.

Memory Overuse: *DrGPUM* [9] monitors GPU memory allocation and deallocation at both the CUDA runtime and third-party framework levels. It detects wasted memory regions that remain unused after allocation or deallocated long after their last access, providing effective optimization strategies for reducing memory peak usage. However, due to the lack of low-level hardware observation, this method does not provide insights into kernel design optimizations or memory access behavior at the instruction level.

B. Memory Access Pattern Detection

Reuse Distance Analysis: Reuse distance analysis has been widely used in GPU cache modeling to predict memory performance [31]–[36]. These studies incorporate detailed cache hierarchy models to evaluate memory locality and reuse patterns. However, as GPU architectures evolve, new cache components are introduced, reducing the reliability of these simulation-based techniques in modern architectures.

Coalescing Rate: NVIDIA Nsight Compute provides hardware counter-based metrics to measure memory coalescing rate by reporting the average number of bytes utilized per memory sector. However, this analysis is performed at the global scope, making it insufficient for identifying inefficient memory access patterns at the instruction level.

Shared Memory Bank Conflict Detection: Gou et al. [37], Horga et al. [38] and others [39], [40] proposed static and dynamic approaches for identifying bank conflicts at compile time and runtime. While these methods effectively detect potential conflicts, they do not provide actionable insights on how to restructure memory access to avoid them, limiting their practical impact on performance optimization.

VIII. CONCLUSIONS AND FUTURE WORK

This paper presents a novel GPU program characterization method and its implementation, CUTHERMO, which provides a comprehensive understanding of memory access patterns in GPU-accelerated applications. CUTHERMO operates on fully optimized binaries without requiring source code, driver, operating system, or hardware modifications. It features a user-friendly heat map GUI that helps users understand memory behaviors in complex kernels. With CUTHERMO, users can optimize their kernels iteratively with guidance and make

informed trade-off decisions. For future work, we plan to incorporate SM ID information and extend the analysis scope to the Grid level to monitor memory access patterns related to hardware bank locations. Additionally, we aim to explore improved data placement strategies and hardware designs for specialized workloads. We will open source CUTHermo.

REFERENCES

- [1] J. Nickolls, I. Buck, M. Garland, and K. Skadron, "Scalable parallel programming with cuda," in *ACM SIGGRAPH 2008 Classes*, ser. SIGGRAPH '08. New York, NY, USA: Association for Computing Machinery, 2008. [Online]. Available: <https://doi.org/10.1145/1401132.1401152>
- [2] J. E. Stone, D. Gohara, and G. Shi, "OpenCL: A parallel programming standard for heterogeneous computing systems," *Computing in Science and Engg.*, vol. 12, no. 3, p. 66–73, may 2010.
- [3] Z. Jia, M. Maggioni, B. Staiger, and D. P. Scarpazza, "Dissecting the nvidia volta gpu architecture via microbenchmarking," *arXiv preprint arXiv:1804.06826*, 2018.
- [4] NVIDIA.Corp. (2025) Nsight compute. [Online]. Available: <https://docs.nvidia.com/nsight-compute/NsightCompute/index.html>
- [5] —. (2025) Compute sanitizer. [Online]. Available: <https://docs.nvidia.com/compute-sanitizer/ComputeSanitizer/index.html>
- [6] K. Zhou, Y. Hao, J. Mellor-Crummey, X. Meng, and X. Liu, "Gvprof: A value profiler for gpu-based clusters," in *SC20: international conference for high performance computing, networking, storage and analysis*. IEEE, 2020, pp. 1–16.
- [7] D. Shen, S. L. Song, A. Li, and X. Liu, "Cudaadvisor: Llvm-based runtime profiling for modern gpus," in *Proceedings of the 2018 International Symposium on Code Generation and Optimization*, 2018, pp. 214–227.
- [8] C. Lattner and V. Adve, "Llvm: A compilation framework for lifelong program analysis & transformation," in *International symposium on code generation and optimization, 2004. CGO 2004*. IEEE, 2004, pp. 75–86.
- [9] M. Lin, K. Zhou, and P. Su, "Drgpum: Guiding memory optimization for gpu-accelerated applications," in *Proceedings of the 28th ACM International Conference on Architectural Support for Programming Languages and Operating Systems, Volume 3*, 2023, pp. 164–178.
- [10] NVIDIA.Corp. (2025) Cuda kernel profiling guide. [Online]. Available: <https://docs.nvidia.com/nsight-compute/ProfilingGuide/index.html>
- [11] O. Villa, M. Stephenson, D. Nellans, and S. W. Keckler, "Nvbit: A dynamic binary instrumentation framework for nvidia gpus," in *Proceedings of the 52nd Annual IEEE/ACM International Symposium on Microarchitecture*, 2019, pp. 372–383.
- [12] NVIDIA.Corp. (2025) Cuda c++ programming guide. [Online]. Available: <https://docs.nvidia.com/cuda/cuda-c-programming-guide/>
- [13] —. (2017) Nvidia tesla v100 gpu architecture. [Online]. Available: <https://images.nvidia.com/content/volta-architecture/pdf/volta-architecture-whitepaper.pdf>
- [14] —. (2025) Cuda c++ best practices guide. [Online]. Available: <https://docs.nvidia.com/cuda/cuda-c-best-practices-guide/>
- [15] M.-K. Yoon, S. Mohan, J. Choi, and L. Sha, "Memory heat map: anomaly detection in real-time embedded systems using memory behavior," in *Proceedings of the 52nd Annual Design Automation Conference*, 2015, pp. 1–6.
- [16] G. Koo, Y. Oh, W. W. Ro, and M. Annamaram, "Access pattern-aware cache management for improving data utilization in gpu," in *Proceedings of the 44th annual international symposium on computer architecture*, 2017, pp. 307–319.
- [17] W. J. Bolosky and M. L. Scott, "False sharing and its effect on shared memory performance," in *USENIX Experiences with Distributed and Multiprocessor Systems (SEDMS IV)*. San Diego, CA: USENIX Association, sep 1993. [Online]. Available: <https://www.usenix.org/conference/sedms-iv/false-sharing-and-its-effect-shared-memory-performance>
- [18] NVIDIA.Corp. (2013) Using shared memory in cuda c/c++. [Online]. Available: <https://developer.nvidia.com/blog/using-shared-memory-cuda-cc/>
- [19] M. Lei, "CUDA-GEMM-Optimization: Optimized matrix multiplication on CUDA," <https://github.com/leimao/CUDA-GEMM-Optimization>, 2023, accessed: 2025-02-23.
- [20] N. Bell and M. Garland, "Implementing sparse matrix-vector multiplication on throughput-oriented processors," in *Proceedings of the Conference on High Performance Computing Networking, Storage and Analysis*, ser. SC '09. New York, NY, USA: Association for Computing Machinery, 2009. [Online]. Available: <https://doi.org/10.1145/1654059.1654078>
- [21] J. Li, Y. Ma, X. Wu, A. Li, and K. J. Barker, "Pasta: a parallel sparse tensor algorithm benchmark suite," *CCF Transactions on High Performance Computing*, vol. 1, pp. 111–130, 2019. [Online]. Available: <https://api.semanticscholar.org/CorpusID:60440602>
- [22] S. Grauer-Gray, L. Xu, R. Searles, S. Ayalasomayajula, and J. Cavazos, "Auto-tuning a high-level language targeted to gpu codes," in *2012 Innovative Parallel Computing (InPar)*, 2012, pp. 1–10.
- [23] Y. Huang, S. Di, G. Li, and F. Cappello, "cuszp2: A gpu lossy compressor with extreme throughput and optimized compression ratio," in *Proceedings of the International Conference for High Performance Computing, Networking, Storage, and Analysis*, ser. SC '24. IEEE Press, 2024. [Online]. Available: <https://doi.org/10.1109/SC41406.2024.00021>
- [24] Z. Fan, W. Chen, V. Vierimaa, and A. Harju, "Efficient molecular dynamics simulations with many-body potentials on graphics processing units," *Computer Physics Communications*, vol. 218, pp. 10–16, 2017. [Online]. Available: <https://www.sciencedirect.com/science/article/pii/S0010465517301339>
- [25] S. G. Sarafianos, K. Das, C. Tantillo, A. D. Clark, J. Ding, J. M. Whitcomb, P. L. Boyer, S. H. Hughes, and E. Arnold, "Crystal structure of hiv-1 reverse transcriptase in complex with a polypurine tract rna:dna," *The EMBO Journal*, vol. 20, no. 6, pp. 1449–1461, 2001. [Online]. Available: <https://www.embopress.org/doi/abs/10.1093/emboj/20.6.1449>
- [26] P. S. Chodrow, N. Veldt, and A. R. Benson, "Hypergraph clustering: from blockmodels to modularity," *Science Advances*, 2021.
- [27] S. Wen, M. Chabbi, and X. Liu, "Redspy: Exploring value locality in software," in *Proceedings of the Twenty-Second International Conference on Architectural Support for Programming Languages and Operating Systems*, 2017, pp. 47–61.
- [28] P. Su, S. Wen, H. Yang, M. Chabbi, and X. Liu, "Redundant loads: A software inefficiency indicator," in *2019 IEEE/ACM 41st International Conference on Software Engineering (ICSE)*. IEEE, 2019, pp. 982–993.
- [29] T. T. Yeh, R. N. Green, and T. G. Rogers, "Dimensionality-aware redundant simt instruction elimination," in *Proceedings of the Twenty-Fifth International Conference on Architectural Support for Programming Languages and Operating Systems*, 2020, pp. 1327–1340.
- [30] K. Zhou, Y. Hao, J. Mellor-Crummey, X. Meng, and X. Liu, "Valueexpert: Exploring value patterns in gpu-accelerated applications," in *Proceedings of the 27th ACM International Conference on Architectural Support for Programming Languages and Operating Systems*, 2022, pp. 171–185.
- [31] C. Nugteren, G.-J. Van den Braak, H. Corporaal, and H. Bal, "A detailed gpu cache model based on reuse distance theory," in *2014 IEEE 20th International Symposium on High Performance Computer Architecture (HPCA)*. IEEE, 2014, pp. 37–48.
- [32] M. Kiani and A. Rajabzadeh, "Rdgc: a reuse distance-based approach to gpu cache performance analysis," *Computing and Informatics*, vol. 38, no. 2, pp. 421–453, 2019.
- [33] Y. Arafat, G. Chennupati, A. Barai, A.-H. A. Badawy, N. Santhi, and S. Eidenbenz, "Gpus cache performance estimation using reuse distance analysis," in *2019 IEEE 38th International Performance Computing and Communications Conference (IPCCC)*. IEEE, 2019, pp. 1–8.
- [34] D. Wang and W. Xiao, "A reuse distance based performance analysis on gpu l1 data cache," in *2016 IEEE 35th International Performance Computing and Communications Conference (IPCCC)*. IEEE, 2016, pp. 1–8.
- [35] C. Li, S. L. Song, H. Dai, A. Sidelnik, S. K. S. Hari, and H. Zhou, "Locality-driven dynamic gpu cache bypassing," in *Proceedings of the 29th ACM on International Conference on Supercomputing*, 2015, pp. 67–77.
- [36] Y. Arafat, A.-H. Badawy, G. Chennupati, A. Barai, N. Santhi, and S. Eidenbenz, "Fast, accurate, and scalable memory modeling of gpgpus using reuse profiles," in *Proceedings of the 34th ACM International Conference on Supercomputing*, 2020, pp. 1–12.
- [37] C. Gou and G. N. Gaydadjiev, "Addressing gpu on-chip shared memory bank conflicts using elastic pipeline," *International Journal of Parallel Programming*, vol. 41, pp. 400–429, 2013.

- [38] A. Horga, A. Rezzine, S. Chattopadhyay, P. Eles, and Z. Peng, “Symbolic identification of shared memory based bank conflicts for gpus,” *Journal of Systems Architecture*, vol. 127, p. 102518, 2022.
- [39] L. Ferranti and J. Boutellier, “Towards algebraic modeling of gpu memory access for bank conflict mitigation,” in *2019 IEEE International Workshop on Signal Processing Systems (SiPS)*. IEEE, 2019, pp. 103–108.
- [40] M. Boyer, K. Skadron, and W. Weimer, “Automated dynamic analysis of cuda programs,” in *Third Workshop on Software Tools for MultiCore Systems*, vol. 33, 2008.